Acta Pharmacologica Sinica

www.nature.com/aps

ARTICLE

Estrogen-dependent depressor response of melatonin via baroreflex afferent function and intensification of PKC-mediated $Na_v1.9$ activation

Di Wu[1,2], Dan Zhao[3], Di Huang[1], Xun Sun[1], Ke-xin Li[1], Yan Feng[1], Qiu-xin Yan[1], Xin-yu Li[1], Chang-peng Cui[1], Hu-die Li[1] and Bai-yan Li[1]

Recent studies suggest that melatonin (Mel) plays an important role in the regulation of blood pressure (BP) via the aortic baroreflex pathway. In this study, we investigated the interaction between the baroreflex afferent pathway and Mel-mediated BP regulation in rats under physiological and hypertensive conditions. Mel (0.1, 0.3, and 1.0 mg/mL) was microinjected into the nodose ganglia (NG) of rats. We showed that Mel-induced reduction of mean arterial pressure in female rats was significantly greater than that in male and in ovariectomized rats under physiological condition. Consistently, the expression of Mel receptors (MTNRs) in the NG of female rats was significantly higher than that of males. In *L*-NAME-induced hypertensive and spontaneously hypertensive rat models, MTNRs were upregulated in males but downregulated in female models. Interestingly, Mel-induced BP reduction was found in male hypertensive models. In whole-cell recording from identified baroreceptor neurons (BRNs) in female rats, we found that Mel (0.1 μM) significantly increased the excitability of a female-specific subpopulation of Ah-type BRNs by increasing the $Na_v1.9$ current density via a PKC-mediated pathway. Similar results were observed in baroreceptive neurons of the nucleus tractus solitarius, showing the facilitation of spontaneous and evoked excitatory post-synaptic currents in Ah-type neurons. Collectively, this study reveals the estrogen-dependent effect of Mel/MTNRs under physiological and hypertensive conditions is mainly mediated by Ah-type BRNs, which may provide new theoretical basis and strategies for the gender-specific anti-hypertensive treatment in clinical practice.

Keywords: melatonin; depressor response; baroreflex affrent pathway; baroreceptor neurons; $Na_v1.9$; PKC

Acta Pharmacologica Sinica (2022) 43:2313–2324; https://doi.org/10.1038/s41401-022-00867-w

INTRODUCTION

Melatonin (Mel) was originally discovered as a pineal gland-derived neurohormone, which mainly regulates circadian rhythm [1, 2]. Numerous studies have indicated that Mel plays an important role in regulating blood pressure (BP) and cardiac diseases in both humans and animal models [3–6]; however, the underlying mechanism is largely elusive. Accumulating evidence has suggested the potential involvement of baroreflex (BRx) control in Mel-mediated BP regulation [7–10]. The key question that has emerged, whether the BRx afferent pathway is merely associated with Mel-mediated BP reduction or a critical contributing regulatory loop, has not been systematically answered.

The BRx pathway is a major neuronal regulatory pathway of BP [11–13]. In the past decade, we have showed that, in adult female rats but not male rats, female-specific subpopulations of myelinated Ah-type baroreceptor (1st order) in the nodose ganglion (NG) and baroreceptive (2nd order) neurons in the nucleus tractus solitarius (NTS) are confirmed. In this afferent pathway, NTS relays BP signals generated from baroreceptor terminals through the aortic depressive nerve (ADN) and NG [14–18]. Among baroreceptor neurons (BRNs) in the NG, Ah-type neurons exclusively express $Na_v1.9$ channels, which are believed to be closely associated with neuroexcitability, which is modulated by PKC phosphorylation [19–22]. Interestingly, several recent reports have suggested unique sex differences in Mel-mediated physiology, such as the expression of Mel receptors, the amount of Mel generated, the rapid release of Mel into the plasma in response to hemorrhage-mediated hypotension, and the Mel-mediated modulation of GABA receptor currents, suggesting an intrinsic correlation between Mel-mediated physiology and BRx-mediated BP regulation [23–27].

To investigate potential mechanism of the Mel/MTNRs-mediated effect through the BRx afferent pathway, we analyzed the expression patterns of MTNRs in BRN subtypes and their specific contributions to the sexual dimorphism of the BRx afferent pathway-mediated control of BP [28–32]. Our findings demonstrated that MTNRs (MT1 and MT2) were highly expressed in the NG neurons of female rats. The direct activation of MTNRs by NG microinjection, Mel dramatically reduced BP (depressor response) in female rats in a concentration-dependent manner.

[1]Department of Pharmacology (State-Province Key Laboratories of Biomedicine-Pharmaceutics of China, Key Laboratory of Cardiovascular Medicine Research, Ministry of Education), College of Pharmacy, Harbin Medical University, Harbin 150081, China; [2]Department of Pharmacy, The Second Affiliated Hospital of Dalian Medical University, Dalian 116023, China and [3]Department of Clinical Pharmacy, The Second Affiliated Hospital of Harbin Medical University, Harbin 150086, China
Correspondence: Bai-yan Li (liby@ems.hrbmu.edu.cn)
These authors contributed equally: Di Wu, Dan Zhao, Di Huang

Received: 23 November 2021 Accepted: 16 January 2022
Published online: 7 February 2022

In addition, our electrophysiological data indicated that Mel-mediated repetitive discharge or spontaneous/evoked excitatory post-synaptic currents (EPSCs) were the most obvious in Ah-type BRNs, and the peak current density of $Na_v1.9$ and PKC phosphorylation were enhanced in the presence of Mel concentration-dependently. These findings strongly suggest that Mel and its receptors play a critical role in autonomic control of BP regulation estrogen-dependently via sexual dimorphism in the BRx afferent function (estrogen-dependent).

MATERIALS AND METHODS

Chemicals

Melatonin (#M5250, Sigma-Aldrich, St. Louis, MO, USA); Luzindole (#L2407, Sigma-Aldrich); PE (#PHR1423, Sigma-Aldrich); Pentobarbital sodium (#P11011, Sigma-Aldrich); SNP (#PHR1423, Sigma-Aldrich); Nω-Nitro-L-arginine methyl ester hydrochloride (*L*-NAME) (#N5751, Sigma-Aldrich); RIPA lysis buffer (#P0013B, Beyotime, Shanghai, China); SDS (#P0013G, Beyotime); Protease Inhibitor Cocktail (#HY-K0010, MedChemExpress, Monmouth Junction, NJ, USA); Phosphatase Inhibitor Cocktail (#04906845001, Roche, Basel, Switzerland); DAPI (#C1005, Beyotime); TRIzol Reagent (#15596-018, Invitrogen, Carlsbad, CA, USA) were ordered directly from the companies. All other chemicals were purchased from the regular commercial sources.

Animals

Ten-week-old male and female Sprague-Dawley (SD) rats weighing 180 ± 20 g were provided by the Experimental Animal Center of Harbin Medical University (grade II). Twelve-week-old male and female Spontaneously hypertensive rats (SHR) and Wistar-Kyoto rats (WKY) weighing 180 ± 20 g were purchased from Beijing Vital River Laboratory Animal Technology. The animals were housed in standard rodent housing at a constant temperature, humidity, and a 12-h light/dark cycle. All animal experiments were performed as per the Guide for the Care and Use of Laboratory Animals (NIH Publication No. 85-23, revised 1996, USA) and granted approval through the Ethics Committee of Harbin Medical University (Harbin, China).

Surgical ovariectomy

Ovariectomy (OVX) was performed following the procedures described previously [28]. Briefly, rats were relaxed with 3% pentobarbital sodium (25 mg/kg, i.p.). The ovaries were excised with forceps through a 1.5 cm incision over both flanks. Plasma estradiol levels in rats have been reported to drop below 5 pg/mL at least two weeks [33]. In this study, the OVX rats were ready to be used for experiments at 4 weeks after the procedures.

Hypertensive models

SHR and WKY rats of both sexes were used as primary hypertensive models and controls ($n = 20$ per group). *L*-NAME-induced secondary hypertension was established using in male SD rats and age-matched females ($n = 20$ per group) as previously described [34].

NG microinjection

The procedures for NG microinjection were described in detail previously [35]. Briefly, rats were anesthetized with 3% pentobarbital sodium (25 mg/kg, i.p.), and placed on a surgical stage in the supine position. A physiological pressure transduced (#MLT 844, AD Instruments, Sydney, Australia) was connected with a cannulation through femoral artery for continuous recording the baseline arterial BP before neck surgery. The left side of NG was carefully exposed and punctured using a precision glass syringe (Hamilton, O.D. × I.D. = 0.31 mm × 0.16 mm, Reno, NEV, USA) affixed with a half-inch 30G stainless steel syringe needle with a 35 °C beveled tip with drug in DMSO (2%). BP was monitored by the NIBP system, in conjunction with a PowerLab system.

Blood pressure measurement

BP, including systolic BP (SBP), diastolic BP (DBP), mean arterial pressure (MAP), and heart rate (HR) were measured by non-invasive tail-cuff plethysmography (BP2010AUL, Softron Biotech., Beijing, China). A heat chamber was set to approximately 37 °C for optimal tail arterial dilatation to allow the assessment of pulsatile pressure. The tail-cuff/sensor was inflated by the system to a maximum pressure of ~250 mmHg, and SBP and pulse were detected using the optical sensor. Throughout the observation, measurements were taken at the same time of the day to minimize the influence of circadian cycles. After the BP was stabilized, the system was used to automatically measure BP ten times, and the average BP was stored in the system.

qRT-PCR

Total RNA was extracted and analyzed according to the manufacturer's protocols (TRIzol, Invitrogen) and converted into cDNA using the Reverse Transcription Kit (Toyobo, Osaka, Japan) on a T100™ thermocycler (Bio-Rad, Hercules, CA, USA). qRT-PCR protocols were performed with a LightCycler 96 instrument (Roche) using SYBR Green MasterMix (Roche). The reactions began with an initial cycle of 95 °C for 10 min followed by 40 cycles of 95 °C for 15 s and 60 °C for 30 s followed by ramping to 72 °C for 30 s. The following primers were used:

MT1: (F) 5′-AAGTCCTGCGGCTTCAGTTTG-3′, (R) 5′-GCCCTGGGCA CATTTGG-3′;

MT2: (F) 5′-TCCTGTGCCACAGATGGATC-3′, (R) 5′-GTCCGAAGCC TCTTTGCAGA-3′;

GAPDH: (F) 5′-AAGAAGGTGGTGAAGCAGGC-3′, (R) 5′-TCCACC ACCCAGTTGCTGTA-3′.

The $2^{-\Delta\Delta Ct}$ method was used to analyze the data, which were normalized and converted to relative mRNA expression. GAPDH served as the normalization gene.

Western blotting

After protein harvest from the tissue of NG or NTS by a cocktail of reagents, a BCA protein assay was used to measure the protein concentration in the supernatant. The same quantity of each protein sample (100 μg) was subjected to 10% SDS-PAGE and then transferred to a nitrocellulose membrane. Primary antibodies: MT1 (1:1000, #A13030, ABclonal, Woburn, MA, USA), MT2 (1:1000, #NLS932, Novus Biologicals, Littleton, CO, USA), PKC (1:1000, #sc-17769, Santa Cruz, Dallas, TX, USA), p-PKC (1:1000, #2261, Cell Signaling Technology, Danvers, MA, USA), GAPDH (1:10,000, #ac002, ABclonal). GAPDH was used as internal controls. Secondary antibodies: goat anti-mouse IgG (1:10,000, #926-32210, LI-COR, Lincoln, NE, USA), goat anti-rabbit IgG (1:10000, #926-32211, LI-COR). The results were visualized and quantified by the Odyssey Infrared Imaging System (#ODY-3149, LI-COR).

Immunohistochemical analysis

The procedures for histological slides of tissue (NG) samples making preparing and pre-processing were described in detail previously [36]. The samples were incubated with primary antibodies against MT1 or MT2 and HCN1with PBS overnight at 4 °C. The antibody against HCN1 (#TA326543, OriGene, Rockville, MD, USA) was used as a fluorescent marker to distinguish myelinated and unmyelinated afferents. The sections were incubated with appropriate secondary antibodies in PBS for 1 h at room temperature. DAPI (DAPI:PBS, 1:1000, Beyotime) was used to stain the nuclei at room temperature for 30 min. Immunofluorescence was observed under 594 nm and 488 nm spectrum, and selected images were taken using a confocal microscope (Olympus Fluo-view 300).

Determination of baroreceptor sensitivity (BRS)
After anesthetization with 3% pentobarbital sodium, the femoral artery was catheterized to measure the alterations in MAP via a pressure transducer, and a venous cannula was used to apply phenylephrine (PE) and sodium nitroprusside (SNP). HR was measured by ECG and recorded by two needle electrodes placed subcutaneously on the lower left forelimb (+) and right hind paw (−). After intravenous injection of different doses of PE and SNP (1, 3 and 10 μg/kg) changes in HR and BP were obtained, and BRS was calculated as ΔHR/ΔMAP (bpm/mmHg).

Electrophysiology
Afferent fiber types of BRNs isolated from the NG of adult female rats were identified by using electrophysiological, pharmacological validation [16] and DiI labeling [17]. The changes in neuronal excitability and the current density of $Na_v1.9$ were evaluated by the whole-cell patch-clamp method in each identified neuron before and after treatment [14]. Spontaneous and evoked EPSCs were also obtained from identified baroreceptive neurons of NTS [18, 37, 38] before and after treatment using brainstem slice preparations.

Statistical analysis
BRS was calculated as ΔHR/ΔMAP in the presence of PE or SNP. Mean fluorescence intensity was measured by ImageJ ProPlus 5.0 (Media Cybernetics). Whole-cell currents of $Na_v1.9$ and EPSCs were recorded using the patch-clamp technique. Clampfit (Molecular Devices, Sunnyvale, CA, USA) was used for initial data readings, and Excel was used for statistical analysis (Microsoft, Northampton, MA, USA). Trace filtering and data graphing were accomplished by Origin (Microsoft). Student's *t*-test and One-way ANOVA were employed where appropriate to compare the differences between and among groups; Dunnett's *t*-test or Fisher's protected least significant difference was conducted *post-hoc* to evaluate pairwise comparisons. The averaged data are presented as the mean ± SD unless specified otherwise. The criterion for statistical significance was set at $P < 0.05$.

RESULTS

Depressor response by direct NG microinjection of Mel under physiological condition
To test whether Mel regulates BP via the baroreceptor reflex pathway, we monitored the alteration of MAP in male, age-matched female and ovariectomized (OVX) rats upon direct NG microinjection of Mel (Fig. 1a). In the vehicle (DMSO) control groups, there were brief and small fluctuations in MAP, but MAP was largely maintained in a control state (Fig. 1b, 1st row). In contrast, MAP was significantly reduced in the Mel-treatment groups when compared to that in the DMSO control groups (Fig. 1b). Interestingly, the current data also showed that the ΔMAP was more dramatic in females than that in males and OVX groups ($P < 0.01$, Fig. 1c), suggesting a unique sex-difference in the Mel-induced depressor response. To test the potential involvement of MTNRs in Mel-mediated BP reduction, a similar experiment in which the Mel receptor antagonist luzindole (2 mg/mL, 3 μL) was administered prior to Mel microinjection was carried out. As expected, luzindole itself did not induce a significant drop in BP ($P > 0.05$ vs. Ctrl), but it greatly reduced the effect of Mel on MAP ($P < 0.01$ vs. Mel alone, Fig. 1d, e). Taking all these data together, we concluded that Mel is a key player in the neurocontrol of BP regulation, likely via the direct activation of MTNRs expressed in the BRx afferent pathway.

MTNRs expression in the NG and NTS
To further investigate the potential involvement of Mel-mediated signaling in the BRx afferent pathway, the expression patterns of MT1 and MT2 in the NG and NTS, in which the cell bodies of the 1st-order BRNs and 2nd-order baroreceptive neurons are located. Either qRT-PCR or Western blot analyses showed that MT1 and MT2 expressions were significantly higher in the NG of female rats than those of male and OVX rats (Fig. 2a–d). The NG contains primary aortic arch BRNs whose projections form synapses with baroreceptive neurons in the NTS, relaying transmission of afferent signals through the ADN. As expected, the NTS had similar MT1 and MT2 expression patterns as the NG (Fig. 2a–d).

To further determine the cellular distribution (cell membrane or cytoplasm) of MT1 and MT2 expression in myelinated A- and Ah-type (HCN1-positive) neurons and unmyelinated C-type (HCN1-negative) neurons, immunofluorescence staining was carried out in the tissue of NG isolated from male, female and OVX rats (Fig. 2e, g). The quantification of the fluorescence intensity indicated that HCN1-positive neurons from females exhibited the highest intensity (Fig. 2f, g). Collectively, the expression patterns of MTNRs in the BRx afferent pathway strongly suggested that Mel-mediated BP regulation likely occurs via MTNRs in the NG and NTS.

Effects of Mel on BP in hypertensive rat models
To further explore the anti-hypertensive effect of Mel, $N^{(\omega)}$-nitro-*L*-arginine methyl ester (*L*-NAME)-induced hypertensive rat models were established (Supplementary Fig. S1). To verify whether the depressor reflex of model rats was impaired, we tested BRS in normal (adult males and females) and hypertensive rats (males and females) by measuring MAP in the presence of PE or SNP. Electrocardiograms (ECGs) were monitored before and after the administration of PE and SNP (Fig. 3a, c, Supplementary Fig. S2). The data demonstrated that the values of ΔHR/ΔMABP, an index of BRS, were dose-dependently decreased in hypertensive models, suggesting an impaired baroreflex (Fig. 3b, d). Through the NG microinjection of Mel, we observed a significant reduction in BP in all tested groups. Intriguingly, the male hypertensive rats showed a more robust anti-hypertensive effect than that observed in the male control group, while the female group showed the opposite trend (Fig. 3e, f). We also tested this unique phenomenon in SHR model. Consistent with the findings described above, Mel-mediated BP reduction was more dramatic in male SHR rats (Supplementary Figs. S3–S5). These data suggested that there was a peculiar gender difference in Mel-mediated BP regulation in the pathophysiological state of hypertension.

Based on the above results, it can be inferred that the gender difference in Mel-mediated BP regulation may be correlated with altered expression of MTNRs in the NG and/or NTS. To this regard, qRT-PCR and immunoblotting were performed to test the expression profiles of MT1/MT2. As shown in Fig. 4a, b, male hypertensive rats exhibited significantly higher MTRs expression when compared with male control rats; however, the inversed expression patterns of these receptors in female hypertensive rats were detected (Fig. 4a–d). Obviously, the immunofluorescence data were consistent well with molecular findings (Fig. 4e, f). Collectively, these data implied that, at least in part, the difference in the response to Mel in male and female hypertensive rats further strengthened the notion that Mel-mediated signaling is involved in the neurocontrol of BP regulation.

Mel mediated neuronal excitation in myelinated Ah-type BRNs
All functional and molecular data indicated that BRx afferent function plays a crucial role in Mel-mediated BP reduction under both physiological and disease conditions. The NG and NTS are the physical locations of the 1st-order BRNs and 2nd-order baroreceptive neurons in the BRx afferent pathway; thus, functional alterations (e.g., neuronal excitability and post-synaptic currents, EPSCs) in these neurons were expected in the presence of Mel. To confirm this, action potentials (APs) were elicited from identified neurons in the NG (Supplementary Fig. S6) isolated from adult female rats using a ramp protocol under the current-clamp configuration. The results showed that both myelinated Ah-type (Fig. 5b) and unmyelinated C-type (Fig. 5c)

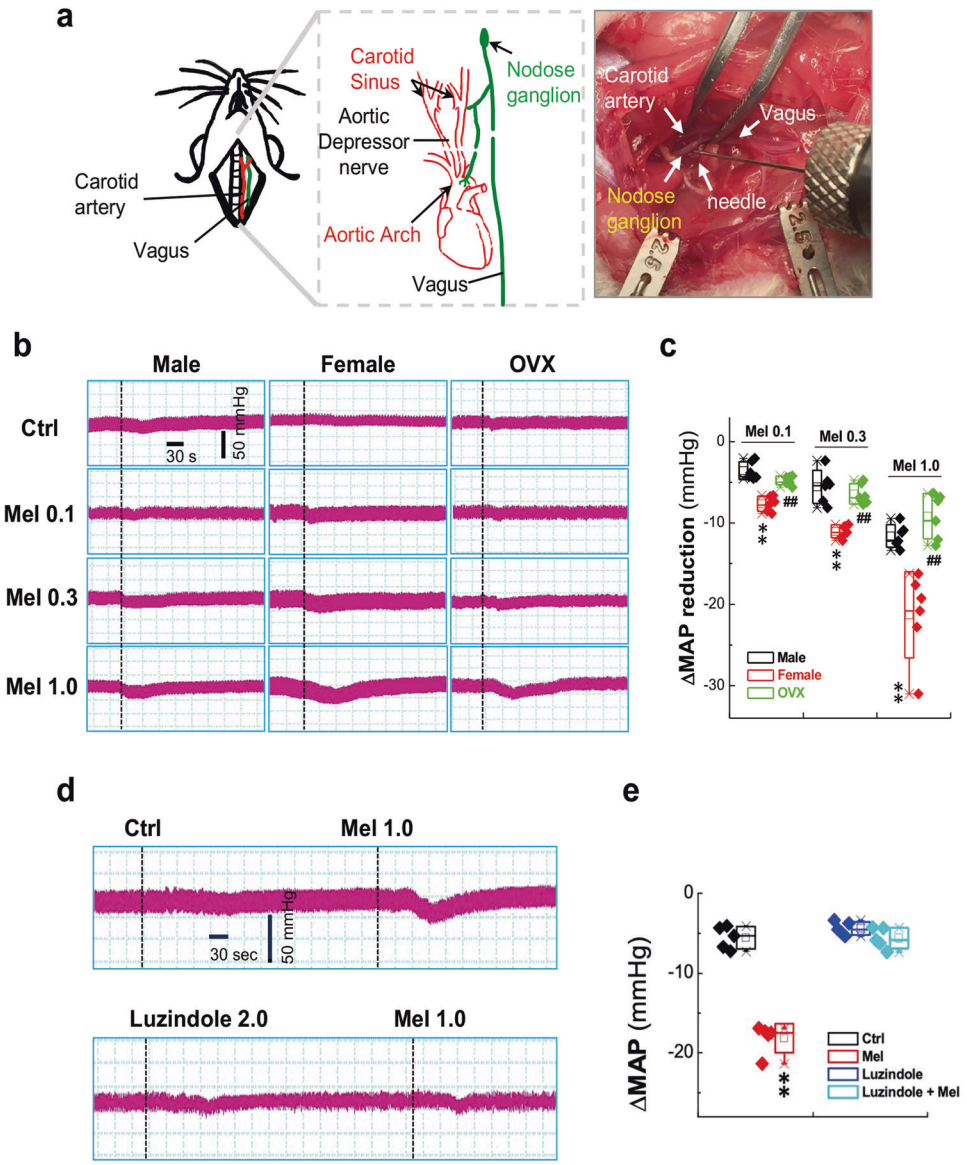

Fig. 1 Melatonin mediated BP reduction by nodose ganglion (NG) microinjection under physiological conditions. The left side of the nodose ganglion (NG) and vagus were dissected and exposed carefully in anesthetic rats. Femoral artery cannulation was performed, and blood pressure (BP) was measured before and after the administration of Mel (0.1, 0.3, and 1.0 mg/mL), DMSO (vehicle control), and luzindole (2.0 mg/mL). **a** Schematic depiction of the NG microinjection. **b**, **c** Representative BP recordings and summary data before and after DMSO and Mel administration in male, female, and ovariectomized (OVX) rats. The dotted line indicates the beginning of treatment. The averaged data are expressed as the mean ± SD. $n = 6$/group. $^{**}P < 0.01$ vs. the male group, $^{\#\#}P < 0.01$ vs. the female group. **d**, **e** Representative BP recordings and summarized data before and after DMSO. Mel or Luzindole+Mel administration in female rats. $^{**}P < 0.01$ *vs.* the Mel group. Of note, Ctrl control, Mel melatonin, Mel 0.1/0.3/1.0 melatonin 0.1/0.3/1.0 mg/mL, Luzindole 2.0 Luzindole 2.0 mg/mL, MAP mean arterial pressure.

neurons were significantly excited in the presence of 0.1 μmol/L Mel (Table 1), which could be completely washed out (Fig. 5a–c). Interestingly, similar events were not observed in myelinated A-types (Fig. 5a).

Based upon our previous reports [19, 39], voltage-gated and tetrodotoxin (TTX)-resistant Na^+ channels ($Na_v1.9$) play a critical role in neuroexcitation in the NG via PKC signaling [21, 22]. PKC is an important regulator of ion channels and membrane excitability in many types of neurons [40]. To test whether $Na_v1.9$ was involved in Mel-induced BRNs excitation, Na^+ currents were recorded in Ah-type BRNs in the presence of 3.0 μmol/L TTX (Supplementary Fig. S7) under voltage-clamp mode, and the results showed that $Na_v1.9$ currents were increased significantly by Mel in a concentration-dependent manner without changes in the voltage-dependent properties of these channels (Fig. 6a–c). The estimated EC_{50} was ~0.294 μmol/L (Fig. 6b). This action of Mel was completely abolished by the addition of Ro31 (a specific inhibitor of PKC) (Fig. 6a), suggesting that PKC signaling is positively involved in Mel-induced $Na_v1.9$ modulation, which was supported by the fact that Mel significantly upregulated phosphorylated PKC expression without affecting total PKC (Supplementary Fig. S8). In addition, a similar observation was confirmed in unmyelinated C-type BRNs but not in myelinated A-type BRNs (data not shown).

Facilitated action of Mel on spontaneous synaptic currents from baroreceptive neurons in the NTS

The 2nd-order neurons in the BRx afferent loop were highly speculated to exhibit spontaneous synaptic currents (miniature potentials) in response to Mel based on the changes in BRNs, the

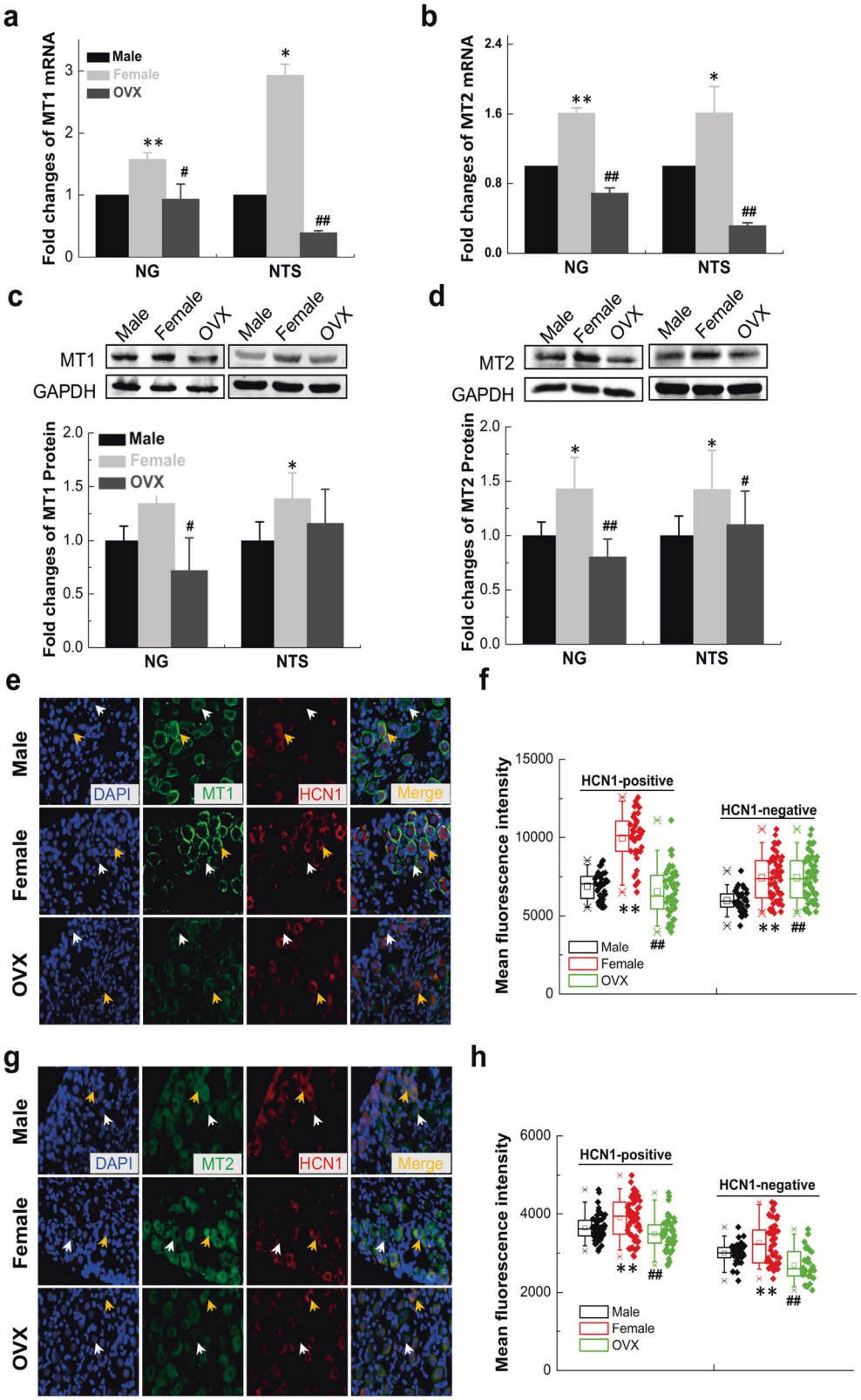

Fig. 2 Mel receptors expression in the nodose ganglia (NG) and nucleus tractus solitarius (NTS). a, **b** Fold changes of MT1/MT2 mRNA in the NG/NTS of adult male, age-matched female and OVX female rats. **c**, **d** Protein expression of MT1/MT2 in the NG/NTS of adult male, age-matched female and OVX female rats. GAPDH served as an internal control. **e**–**h** Immunohistochemical staining for MT1/MT2. Tissues for staining were collected from the NG of adult male, age-matched female, and OVX rats. Nuclei, hyperpolarization-activated channels specifically expressed on myelinated afferents (HCN1-positive), and MT1/MT2 were labeled with antibodies against DAPI (blue), HCN1 (red), and MT1/MT2 (green), respectively. The white arrow indicates neurons with unmyelinated afferents (HCN1-negative), and the yellow arrow indicates neurons with myelinated afferents (HCN1-positive). The averaged data are presented as the mean ± SD. $^{*}P < 0.05$, $^{**}P < 0.01$ vs. the male group; $^{\#}P < 0.05$, $^{\#\#}P < 0.01$ vs. the female group.

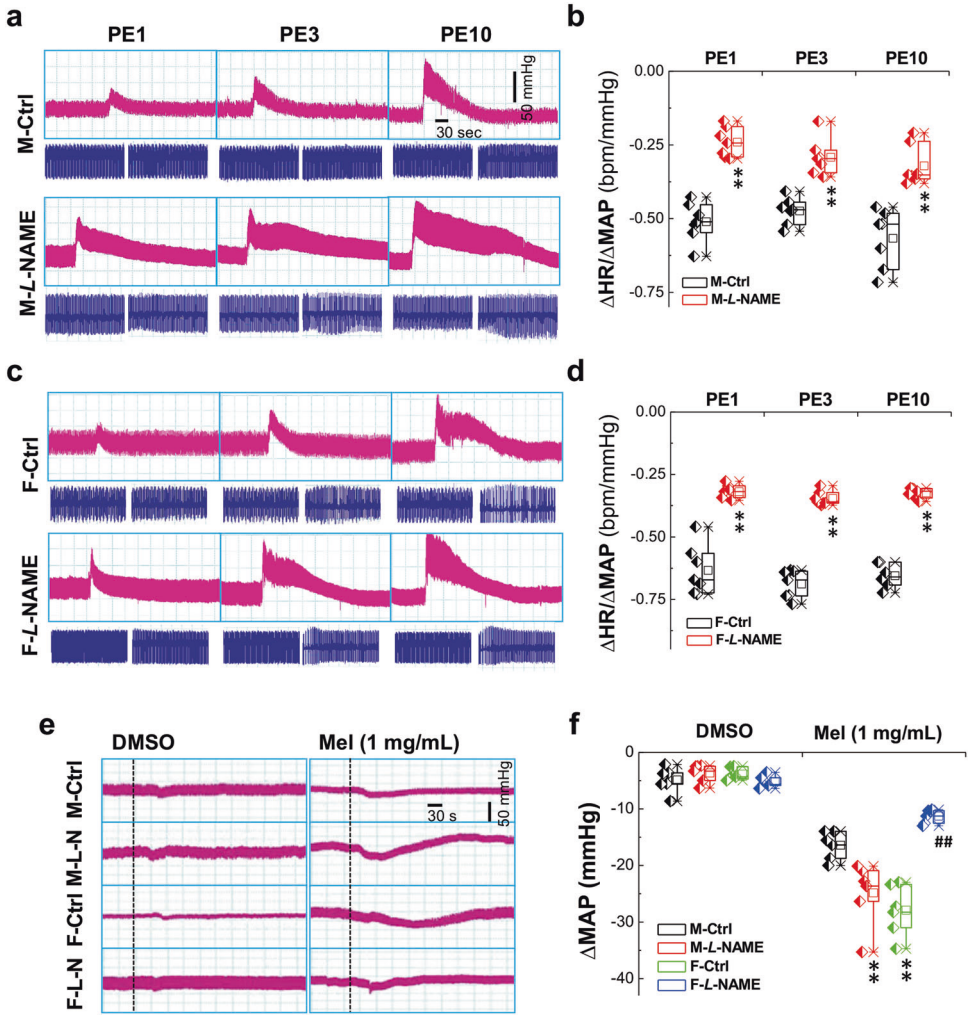

Fig. 3 Changes in baroreceptor sensitivity (BRS) and the effects of Mel on BP under hypertensive conditions in *L*-NAME model rats. a–d Femoral artery catheterization was applied to measure the ΔMAP, and venous cannula was used for the administration of PE. Representative MAP recordings collected from M-Ctrl, M-*L*-NAME, F-Ctrl, and F-*L*-NAME rats in the presence of 1, 3, and 10 μg/kg PE (pink traces). Concomitant recordings of HR (blue traces) and blood pressure (upper panel) were presented. The summary of changes in BRS (ΔHR/ΔMAP, bpm/mmHg) upon treatment with PE at different concentrations in each group (bottom panel); **e**, **f** Representative blood pressure recordings before and after DMSO and Mel (1 mg/mL) administration in M-Ctrl, M-*L*-NAME, F-Ctrl, and F-*L*-NAME rats. The dotted line indicates the beginning of treatment (upper panel). Summary data of ΔMAP values before and after DMSO and melatonin microinjection (bottom panel). The averaged data are presented as the mean ± SD. $n = 7$. $^{**}P < 0.01$ vs. the M-Ctrl or F-Ctrl group; $^{\#\#}P < 0.01$ vs. the F-Ctrl group. Of note, M-Ctrl male control, M-*L*-NAME male *L*-NAME, F-Ctrl female control, F-*L*-NAME female *L*-NAME, HR heart rate, MAP mean arterial pressure, PE phenylephrine, Mel melatonin.

1st-order neurons. To test this assumption, we investigated the changes in spontaneous synaptic currents prior to and after treatment with 0.1 μmol/L Mel. In myelinated Ah-type baroreceptive neurons of brainstem slice preparation (Supplementary Fig. S9), the total number of miniature potentials was dramatically increased by Mel, and this effect was completely blocked in the presence of Ro31 (Fig. 7a–c). Intriguingly, by looking into the dynamic signatures of these spontaneous synaptic currents, including the rise and decay times (Supplementary Fig. S10), the number of miniature potentials representing EPSCs, but not those representing inhibitory-post-synaptic currents (IPSCs), was significantly increased in Ah-type neurons (Fig. 7g) [32]. This strongly suggested that the release of the excitatory neurotransmitter glutamate from the terminals of the 1st-order BRNs had a dominant role in BRx and BP reduction mediated by Mel through BRx afferent function, which was supported by the notion that NG microinjection of Mel induced a decrease in BP (Fig. 1b). Due to their specific distribution in female, Ah-type baroreceptive neurons are likely the key players in Mel-mediated depressor response via the BRx afferent pathway. Although A-type neurons are also myelinated ones of the NTS, the corresponding alterations were not detected in the presence of Mel.

In addition, Mel induced identical but less significant changes in the number of miniature potentials representing either EPSCs or IPSCs in C-types (Fig. 7d–f), implying that they are unlikely to be important for the depressor response induced by Mel, simply because that (1) both EPSCs and IPSCs (Fig. 7h) were altered in the similar manner, so their effects (excitatory and inhibitory) may be counteracted partially and led to less action from efferent loop even though the total members were increased; (2) the equal distribution and similar function of C-types were confirmed clearly in both male and female rats.

Effects of Melon EPSCs and IPSCs in baroreceptive neurons of the NTS

To further confirm the role of Mel in the 2nd-order neurons, EPSCs were evoked by solitary tract stimulation in baroreceptive neurons, and the areas under the curve (AUCs) of EPSCs were evaluated in A-, Ah- and C-types (Fig. 8a–c). After synaptic desensitization by application of cyclothiazide (CTZ), the release

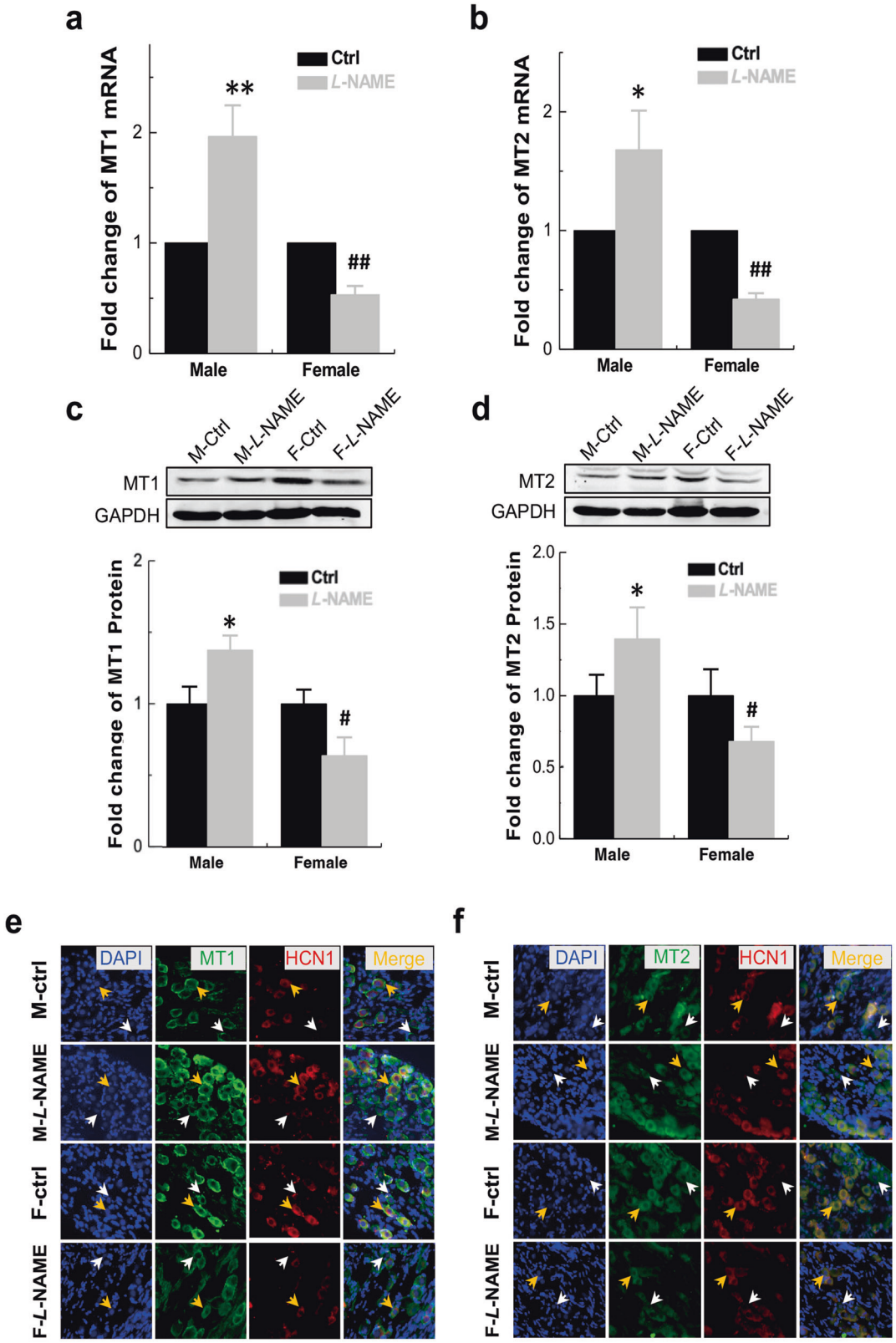

Fig. 4 Downregulation of Mel receptors (MRs) in the nodose ganglia (NG) under hypertensive conditions. a–d MT1/MT2 mRNA and protein expression changes in secondary hypertensive model rats (M-Ctrl, M-*L*-NAME, F-Ctrl, and F-*L*-NAME). **e**, **f** Immunohistochemical staining for MT1/MT2. Staining was performed in the NG of M-Ctrl, M-*L*-NAME, F-Ctrl and F-*L*-NAME rats. Nuclei, hyperpolarization-activated channels specifically expressed on myelinated afferents (HCN1-positive), and MT1/MT2 were labeled with antibodies against DAPI (blue), HCN1 (red), and MT1/MT2 (green), respectively. The white arrow indicates neurons with unmyelinated afferents (HCN1-negative), and the yellow arrow indicates neurons with myelinated afferents (HCN1-positive). The data are presented as the mean ± SD. $^{*}P < 0.05$, $^{**}P < 0.01$ vs. M-Ctrl; $^{\#}P < 0.05$, $^{\#\#}P < 0.01$ vs. F-Ctrl. Of note, M-Ctrl male control, M-*L*-NAME male *L*-NAME, F-Ctrl female control, F-*L*-NAME female *L*-NAME, Ctrl control.

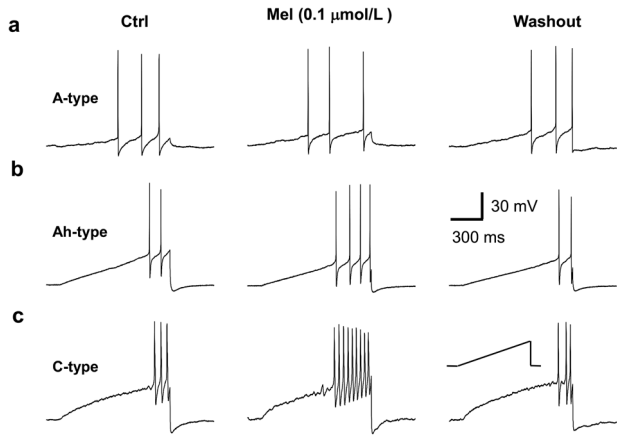

Fig. 5 Effect of Mel on neuronal excitability. Action potentials were elicited by a ramp protocol under current-clamp configuration. The frequency of APs in myelinated A- and Ah-type and unmyelinated C-type BRNs isolated from adult female rats was evaluated before and after the administration of 0.1 μmol/L Mel. **a** A representative recording from A-type neurons before and after Mel administration. **b** A representative recording from Ah-type neurons before and after Mel administration; **c** A representative recording from C-type neurons before and after Mel administration. The scale bars in (**b**) apply to all recordings. Of note, Ctrl control, Mel melatonin.

Table 1. Effects of Mel on the total events of spontaneous EPSCs, IPSCs, and ratio of EPSCs/IPSCs recorded from myelinated Ah-type and unmyelinated C-type baroreceptive neurons of NTS brainstem slices in adult female rats.

	Total events	# of EPSCs	# of IPSCs	EPSCs/IPSCs
	Ah-type baroreceptive neurons, *n* = 6			
Control	92.4 ± 36.1	69.2 ± 26.4	32.4 ± 11.7	>2.0
0.1 μmol/L Mel	167.7 ± 45.8**	115.1 ± 31.4**	55.8 ± 23.6**	>2.0
+PKC blocker	66.5 ± 34.9##	52.8 ± 22.2##	27.9 ± 8.7##	<2.0
	C-type baroreceptive neurons, *n* = 8			
Control	56.1 ± 13.2	27.8 ± 7.7	30.3 ± 7.6	<1.0
0.1 μmol/L Mel	75.7 ± 15.1*	40.4 ± 9.2**	31.8 ± 9.6	>1.0
+PKC blocker	49.6 ± 10.5#	23.4 ± 6.9#	29.7 ± 8.1	<1.0

Mel melatonin.
*$P < 0.05$, **$P < 0.01$ vs. Control group; #$P < 0.05$, ##$P < 0.01$ vs. 0.1 μmol/L Mel group.

and clearance of glutamate from the pre-synaptic membrane could be evaluated by measuring the AUC and the decay time constant. The results showed that the total AUC was robustly increased by 0.1 μmol/L Mel in Cap-insensitive Ah-type neurons (Fig. 8b, d) on top of CTZ along with increased decay time constant, suggesting significant release of the excitatory neurotransmitter glutamate from the terminal of the 1st-order BRNs in the presence of Mel and slowed clearance of glutamate from the synaptic cleft, which led to BP reduction through the BRx afferent pathway in female rats. A similar action of Mel on C-type neurons was also confirmed under this experimental condition (Fig. 8c, d) [32]. As expected, a significant alteration in the AUC was not observed in Cap-insensitive A-type baroreceptive neurons, presumably because of negative $Na_v1.9$ expression [19].

DISCUSSION

The major contribution of this observation is to demonstrate for the first time that Mel could induce the depressor response

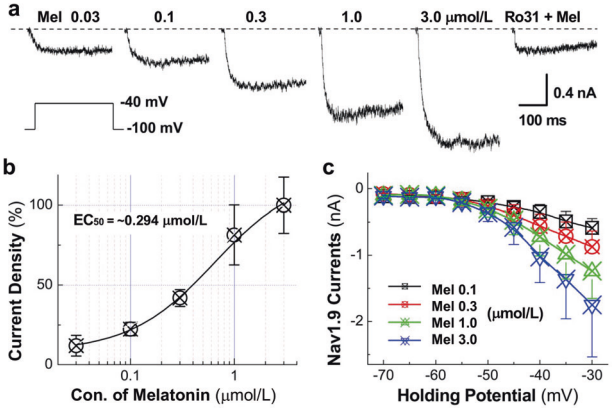

Fig. 6 Alterations in voltage-gated Na^+ channels ($Na_v1.9$) in the presence of Mel. $Na_v1.9$ currents were recorded from myelinated Ah-type BRNs isolated from adult female rats in the presence of 1 mmol/L tetrodotoxin (TTX) under voltage-clamp mode. Mel and/or Ro31 (a specific inhibitor of PKC) was applied through a bath perfusion system at a rate of ~1.0 mL/min. The current amplitude was collected at 400 ms. **a** Representative recordings of $Na_v1.9$ with or without the administration of Mel alone or Mel with 3.0 μmol/L Ro31 are shown. **b** A concentration-response curve of Mel was created, and the 50% effective concentration (EC_{50}) was estimated as ~0.294 μmol/L; **c** The current-voltage relationship under different concentrations of Mel (0.03–3 μmol/L). The data are presented as the mean ± SD. $n = 6$-11 complete recordings from each group. Of note, Mel melatonin, Con. concentration.

estrogen- and concentration-dependently via direct activation of Ah-type BRNs in the NG. Moreover, higher expression of Mel receptors in these neurons triggers the PKC phosphorylation that intensifies $Na_v1.9$, which further facilitates synaptic transmission to baroreceptive neurons in the NTS, eventually to balance the autonomic control of BP regulation toward the enhancement of parasympathetic tone and lead the depressor recompense.

Mel, the primary circadian hormone, can affect structures in the central nervous system as well as cellular function in the rest of the body, for example, heart and vessels [41, 42]. In many cases, Mel effects are ambiguous, due to its capability pass the cell membrane directly or through the specific membrane receptors [43]. A direct effect of Mel on BP has been described. Continuous Mel infusion was also effective to reduce BP of hypertensive rats [44] and hypertensive and normotensive humans [5, 45, 46]. In our study, the results indicate that acute microinjection of Mel into the NG reduced BP both in normotensive and hypertensive rats. In particular, this BP reduction is more remarkable in female rats compared with male and OVX rats. It's noting that this reduction was almost abolished by the Mel receptors antagonist (luzindole) before Mel administration, strongly suggesting the direct involvement of the BRx afferent pathway in Mel-mediated BP reduction through the direct activation of Mel receptors expressed in the BRx afferent pathway (NG and NTS). Luzindole acts as a Mel receptor antagonist, with an approximately 11- to 25-fold greater affinity for MT2 than that for MT1 [47]. We could not determine with certainty at this point the specific receptors that Mel activates to exert its anti-hypertensive effect; this will require additional analyses of MT1- or MT2-specific knockout models in the future.

Sympathetic overactivation contributes to the pathogenesis of both experimental and human hypertension. It's reported that the BRx control of HR and renal sympathetic nerve activity were improved after Mel treatment in the hypertensive rats [48]. It has been previously reported that the BRS could be improved by chronic Mel treatment in SHR rats [8]. In our study, the *L*-NAME-induced hypertensive (secondary hypertension) and SHR (primary hypertension) model rats were employed to investigate the effects of Mel on alteration in BP and Mel receptor expression. The

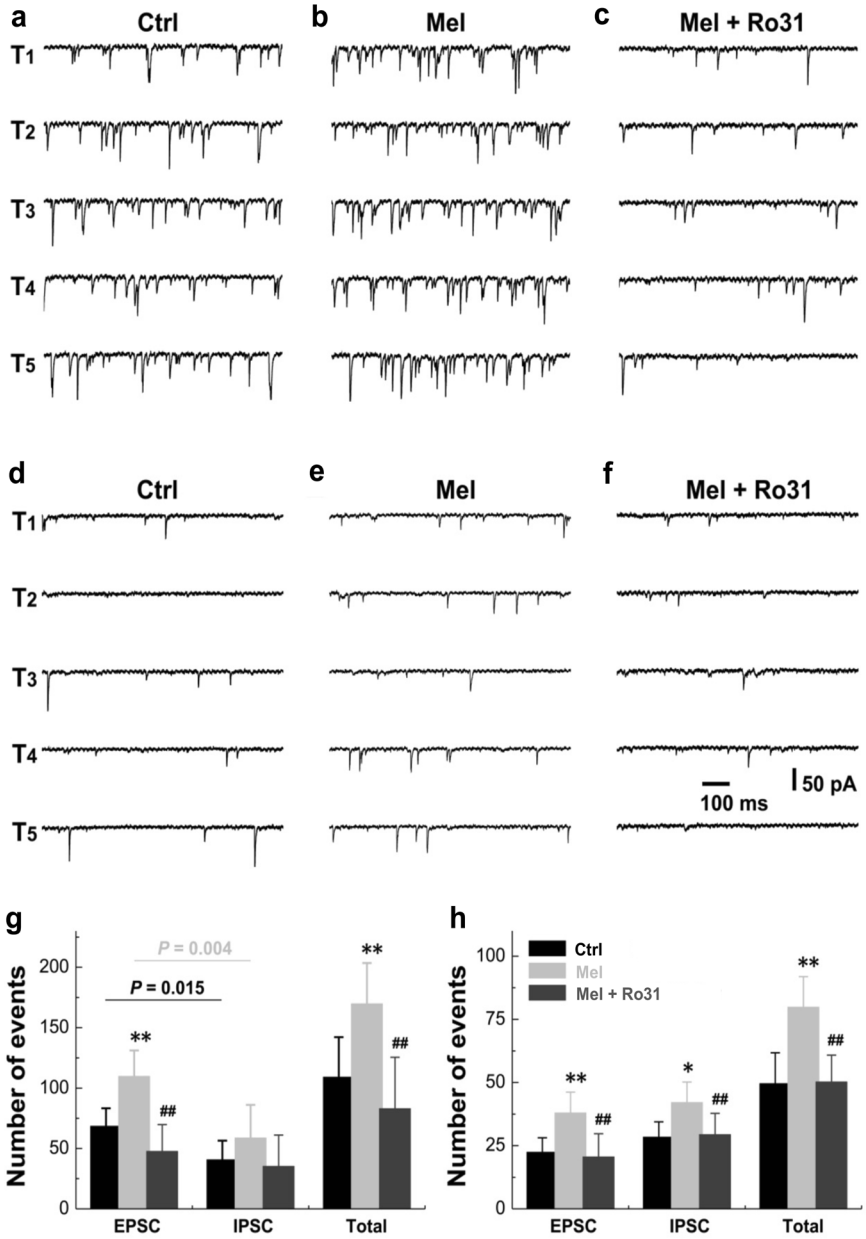

Fig. 7 Changes in spontaneous miniature potentials recorded from the nucleus tractus solitarius (NTS) from brainstem slices of adult female rats. Five consecutive traces of miniature potentials were recorded from each identified baroreceptive neuron of the NTS before and after the administration of 0.1 μmol/L Mel or Mel with 3.0 μmol/L Ro31 (a specific inhibitor of PKC). **a**–**c** Representative recordings from myelinated Ah-type baroreceptive neurons of the NTS upon control (Ctrl) or treatment with Mel or Mel+Ro31. **d**–**f** Representative recordings from myelinated C-type baroreceptive neurons of the NTS upon control (Ctrl) treatment or treatment with Mel or Mel+Ro31. **g**, **h** Summary data of total miniature potentials, excitatory post-synaptic currents (EPSCs), and inhibitory post-synaptic currents (IPSCs) in Ah- or C-type neurons. The averaged data are presented as the mean ± SD. $n = 8$-10 complete recordings from each group. $^{*}P < 0.05$, $^{**}P < 0.01$ vs. Ctrl; $^{\#\#}P < 0.01$ vs. Mel group. Of note, Ctrl control, Mel melatonin.

impaired BRS observed in both model rats confirmed that BRx afferent function is critical for the development of hypertension. Interestingly, compared with control rats (SD rats or WKY treated with Mel), BP reduction was observed in male *L*-NAME-induced rats and male SHR rats after NG microinjection of Mel, rather than female *L*-NAME-induced rats or SHR rats underwent similar treatment; however, the BP reduction observed in female controls treated with Mel was less than half that observed in both hypertensive models treated with Mel (Fig. 3f and Supplementary Fig. S5b). These functional observations were consistent with the mRNA and protein expression profiles in the NG, which showed that MT1 and MT2 were upregulated and downregulated, respectively, in male and female model rats. Even this finding could not be explained under the current experimental conditions, and further work is necessary.

Collectively, our findings clearly indicate that sexually dimorphic expression of Mel receptors is the plausible explanation for the Mel-mediated sexual dimorphic depressor response; however, it is difficult to verify which types of BRNs are more responsible. Although single-cell qRT-PCR can help to determine the expression of MT1/MT2 at the cellular level, the significant variation between cells increases the risk of false positives; therefore, tests of neuroexcitability in BRNs is the best way to reach our goal [16, 23, 28, 29, 31, 49]. In the presence of 0.1 μmol/L Mel, the AP

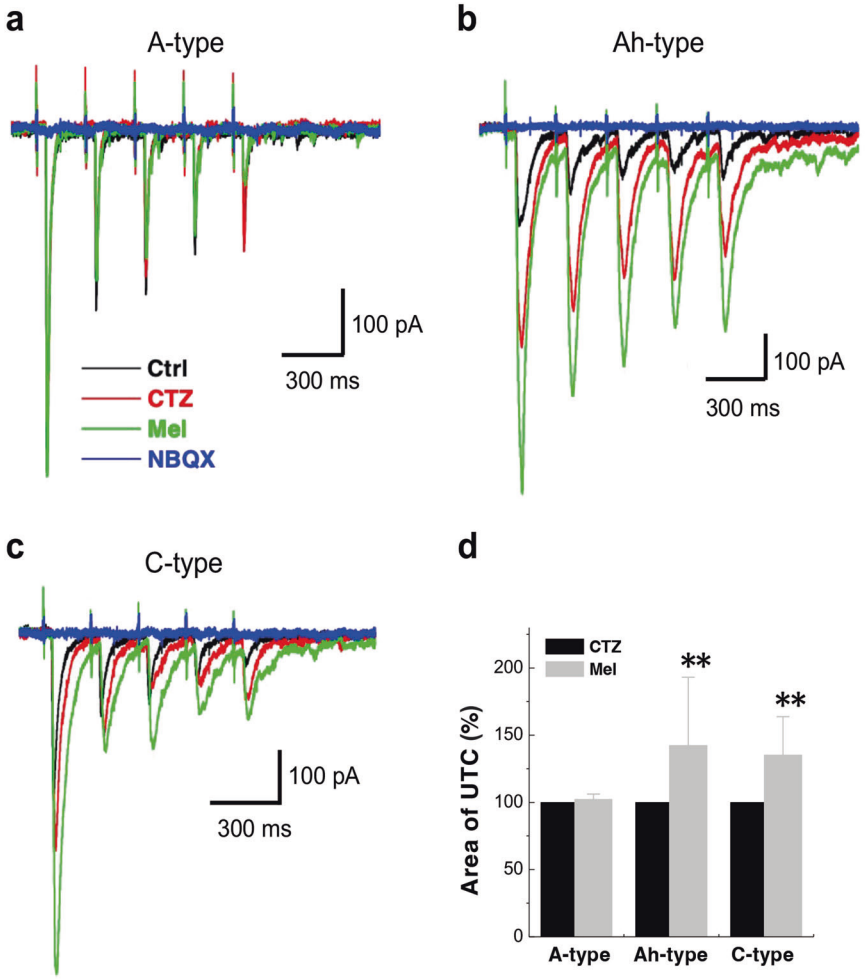

Fig. 8 Changes in evoked excitatory post-synaptic currents (EPSCs) in the 2nd-order baroreceptive neurons of the nucleus tractus solitarius (NTS) in brainstem slices from adult female rats. EPSCs were evoked by solitary track stimulation (▲) with a 5-shock protocol. For fiber type classification, 100 nmol/L capsaicin (Cap) was bath-applied at the end of recording, and myelinated A- and Ah-type and unmyelinated C-type BRNs were identified and showed delayed excitation. A-type: Cap-insensitive without delayed excitation; Ah-type: Cap-insensitive with slightly delayed excitation; C-type: Cap-sensitive with significantly delayed excitation. For evaluation, the sum of the area under the curve (AUC) of EPSCs (pA*ms) was determined at each time point and multiplied by the actual value of EPSCs from 20 ms before to 20 ms after the stimulation. For comparison, the tested value was normalized, and the % changes are presented. CTZ (100 μmol/L) was applied before Mel to prevent the rapid desensitization of aminomethylphosphonic acid (AMPA) receptor activation, and NBQX (50 nmol/L) was also applied after Mel to further confirm the activation of AMPA. **a**–**c** Representative recordings from of A-, Ah-, and C-type baroreceptor neurons in the presence or absence of melatonin. **d** The averaged data are presented as the mean ± SD. $n = 13$ complete recordings from 7 brainstem slices. $^{**}P < 0.01$ vs. CTZ. Of note, Ctrl control, Mel melatonin, CTZ cyclothiazide, NBQX 2,3-dihydroxy-6-nitro-7-sulfamoylbenzo[f]quinoxaline-2,3-dione.

discharge frequency and firing threshold under the ramp protocol were not affected in A-type neurons, but increased nearly 100% and reduced from −19.6 ± 4.2 mV to −32.2 ± 3.16 mV ($P < 0.01$), respectively, in Ah-type BRNs. Although an increased AP frequency was also observed in C-type neurons, the change in the AP firing threshold was not detected, indicating that both Ah- and C-type neurons, rather than A-type neurons, are involved in Mel-induced depressor response (Fig. 5a–c). Considering the female-specific distribution of myelinated Ah-type BRNs, we believe that Ah-type BRNs are very likely the key player in the sexual dimorphism in Mel-mediated BP reduction [15, 16].

The underlying ion channel mechanism to cause an increased excitability is of great significance to further understanding of the anti-hypertensive properties of Mel. Based on our previous observations, Ah-type neurons functionally express not only $Na_v1.9$ [19] but also BK-KCa [28, 50], which is commonly observed in C-type neurons [18, 37, 51, 52]. By looking into AP waveforms, significant alternations before and after Mel were not verified, suggesting the negative involvement of BK-type KCa. Therefore, $Na_v1.9$ would be a direct target for Mel-mediated neuroexcitation via its receptor activation, particularly in Ah-type neurons [21]. As expected, Mel caused voltage- and concentration-dependent increases in the current density of $Na_v1.9$ with an estimated $EC_{50} = \sim 0.294$ μmol/L in identified Ah-type BRNs. Obviously, the effect of Mel on neuroexcitability was mediated by the PKC signaling pathway after MT1/MT2 activation, which is consistent with the data from these experiments and others showing the direct action of the BRx pathway [7, 53]. Although the PKC binding site on $Na_v1.9$ was not determined in the current investigation, identifying it would not change our conclusion.

The NTS is the cardiovascular center in the brainstem and houses the 2nd-order baroreceptive neurons in the BRx afferent pathway; therefore, it plays a crucial role in relaying BRx afferent signals arising from baroreceptor terminals through BRNs in the NG. Based on theory and data from BRNs, spontaneous and evoked EPSCs could be altered by Mel in Ah-type baroreceptive

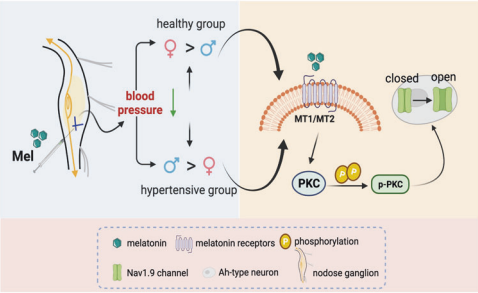

Fig. 9 Graphic mechanism of melatonin-mediated BP reduction via receptor activation and PKC phosphorylation in the BRx afferent pathway. This study found that the microinjection of Mel into the nodose ganglia of healthy SD rats can lower BP and that females are more sensitive than males to this anti-hypertensive effect. Moreover, a unique population of neurons, Ah-type neurons were found in the female rats and we suspect that these neurons play an important role in lowering BP. However, under pathological conditions of hypertension, we found that the hypotensive effect of Mel was reversed in male and female rats; that is, male hypertensive rats were more sensitive than female hypertensive rats. Through molecular biology experimental techniques, we demonstrated that male rats with high BP have elevated receptor levels compared to those of females. Through electrophysiological experiments, we demonstrated that Mel activates and then phosphorylates protein kinase C by binding to MTNRs and finally activates $Na_v1.9$ channels to exert an antihypertensive effect.

neurons as well as C-type neurons, but not A-type neurons, via PKC signaling. This ratiocination is in accordance with our observations in brainstem slice recordings. Firstly, the changes in spontaneous events were not detected in A-types, implying that they are not players. Secondly and most importantly, spontaneous EPSCs, but not IPSCs, increased significantly in Ah-type baroreceptive neurons, indicating that the net change in EPSCs/IPSCs favored the BRx activation and consequent depressor response induced by Mel. Finally, even though total spontaneous events increased in C-type neurons, both EPSCs and IPSCs increased to a similar degree, suggesting that the outcomes in C-types were balanced out and would not affect BRx activity presumably. Accordingly, the alteration of evoked EPSCs in Ah-type baroreceptive neurons by Mel was not surprising, and the increase in the area under the curve of evoked EPSCs demonstrated increased glutamate release and subsequent Mel-mediated BP reduction.

In summary, this current investigation have demonstrated that the BRx afferent pathway plays an important role in Mel-mediated depressor response via direct baroreceptor and Mel receptor activations under both physiological and hypertensive conditions. Mel-mediated neuroexcitation of Ah-type BRNs in the NG and corresponding changes in spontaneous/evoked EPSCs in baroreceptive neurons in the NTS could lead to the release of glutamate and eventually BP reduction. Moreover, PKC phosphorylation and the increase of $Na_v1.9$ expression are major mechanisms. These data provide direct evidence that Mel plays a crucial role in the neurocontrol of BP regulation via the BRx afferent pathway and may open new opportunities for clinical management of hypertension with consideration of gender (Fig. 9).

ACKNOWLEDGEMENTS

This study was supported by research grants from the National Natural Science Foundation of China (81573431, 81971326, and 31871175). This work was especially dedicated to and commemorated for Professor/Dr. Wen-fen Chu for his outstanding performance and unselfish contribution to the Basic Medical Science as well as his personal character during his professional career at the Department of Pharmacology, Harbin Medical University. These authors would like also thank Dr. Rong Huo and Dr. Ning Wang for their helps and valuable inputs in qRT-PCR techniques and data interpretations.

AUTHOR CONTRIBUTIONS

DW, DZ, DH, and BYL designed the study and interpreted the results. DW, DH, XS, YF performed molecular expression experiments. KXL, QXY, XYL contributed to collecting animal samples. DW and BYL conducted the patch-clamp experiments. DH, CPC, and HDL are responsible for correcting the proofs. DW, DZ, and BYL drafted and reviewed the manuscript. DW and BYL finalized the manuscript. BYL and DZ provided research funding.

ADDITIONAL INFORMATION

Supplementary information The online version contains supplementary material available at https://doi.org/10.1038/s41401-022-00867-w.

Competing interests: The authors declare no competing interest.

REFERENCES

1. Auld F, Maschauer EL, Morrison I, Skene DJ, Riha RL. Evidence for the efficacy of melatonin in the treatment of primary adult sleep disorders. Sleep Med Rev. 2017;34:10–22.
2. Hardeland R, Pandi-Perumal SR, Cardinali DP. Melatonin. Int J Biochem Cell Biol. 2006;38:313–6.
3. Simko F, Baka T, Krajcirovicova K, Repova K, Aziriova S, Zorad S, et al. Effect of melatonin on the renin-angiotensin-aldosterone system in *L*-NAME-induced hypertension. Molecules. 2018;23:265.
4. Grossman E, Laudon M, Yalcin R, Zengil H, Peleg E, Sharabi Y, et al. Melatonin reduces night blood pressure in patients with nocturnal hypertension. Am J Med. 2006;119:898–902.
5. Grossman E, Laudon M, Zisapel N. Effect of melatonin on nocturnal blood pressure: meta-analysis of randomized controlled trials. Vasc Health Risk Manag. 2011;7:577–84.
6. Smolensky MH, Hermida RC, Portaluppi F. Circadian mechanisms of 24-hour blood pressure regulation and patterning. Sleep Med Rev. 2017;33:4–16.
7. Campos LA, Cipolla-Neto J, Michelini LC. Melatonin modulates baroreflex control via area postrema. Brain Behav. 2013;3:171–7.
8. Girouard H, Denault C, Chulak C, de Champlain J. Treatment by n-acetylcysteine and melatonin increases cardiac baroreflex and improves antioxidant reserve. Am J Hypertens. 2004;17:947–54.
9. Kitajima T, Kanbayashi T, Saitoh Y, Ogawa Y, Sugiyama T, Kaneko Y, et al. The effects of oral melatonin on the autonomic function in healthy subjects. Psychiatry Clin Neurosci. 2001;55:299–300.
10. Baker J, Kimpinski K. Role of melatonin in blood pressure regulation: an adjunct anti-hypertensive agent. Clin Exp Pharmacol Physiol. 2018;45:755–66.
11. Hildebrandt DA, Irwin ED, Lohmeier TE. Prolonged baroreflex activation abolishes salt-induced hypertension after reductions in kidney mass. Hypertension. 2016;68:1400–6.
12. Mar PL, Nwazue V, Black BK, Biaggioni I, Diedrich A, Paranjape SY, et al. Valsalva maneuver in pulmonary arterial hypertension: susceptibility to syncope and autonomic dysfunction. Chest. 2016;149:1252–60.
13. Shi Z, Li B, Brooks VL. Role of the paraventricular nucleus of the hypothalamus in the sympathoexcitatory effects of leptin. Hypertension. 2015;66:1034–41.
14. Li BY, Schild JH. Patch clamp electrophysiology in nodose ganglia of adult rat. J Neurosci Methods. 2002;115:157–67.
15. Li BY, Qiao GF, Feng B, Zhao RB, Lu YJ, Schild JH. Electrophysiological and neuroanatomical evidence of sexual dimorphism in aortic baroreceptor and vagal afferents in rat. Am J Physiol Regul Integr Comp Physiol. 2008;295:R1301–10.
16. Li BY, Schild JH. Electrophysiological and pharmacological validation of vagal afferent fiber type of neurons enzymatically isolated from rat nodose ganglia. J Neurosci Methods. 2007;164:75–85.
17. Lu XL, Xu WX, Yan ZY, Qian Z, Xu B, Liu Y, et al. Subtype identification in acutely dissociated rat nodose ganglion neurons based on morphologic parameters. Int J Biol Sci. 2013;9:716–27.
18. Zhang YY, Yan ZY, Qu MY, Guo XJ, Li G, Lu XL, et al. KCa1.1 is potential marker for distinguishing Ah-type baroreceptor neurons in NTS and contributes to sex-specific presynaptic neurotransmission in baroreflex afferent pathway. Neurosci Lett. 2015;604:1–6.
19. Qiao GF, Li BY, Zhou YH, Lu YJ, Schild JH. Characterization of persistent TTX-R Na^+ currents in physiological concentration of sodium in rat visceral afferents. Int J Biol Sci. 2009;5:293–7.
20. Huang J, Vanoye CG, Cutts A, Goldberg YP, Dib-Hajj SD, Cohen CJ, et al. Sodium channel NaV1.9 mutations associated with insensitivity to pain dampen neuronal excitability. J Clin Invest. 2017;127:2805–14.
21. Copel C, Osorio N, Crest M, Gola M, Delmas P, Clerc N. Activation of neurokinin 3 receptor increases Na(v)1.9 current in enteric neurons. J Physiol. 2009;587:1461–79.

22. Kurowski P, Grzelka K, Szulczyk P. Ionic mechanism underlying rebound depolarization in medial prefrontal cortex pyramidal neurons. Front Cell Neurosci. 2018;12:93.
23. Howard CM, Lutterschmidt DI. The effects of melatonin on brain arginine vasotocin: relationship with sex and seasonal differences in melatonin receptor type 1 in green treefrogs (Hyla cinerea). J Neuroendocrinol. 2015;27:670–9.
24. Viswanathan M, Laitinen JT, Saavedra JM. Differential expression of melatonin receptors in spontaneously hypertensive rats. Neuroendocrinology. 1992;56:864–70.
25. Santhi N, Lazar AS, McCabe PJ, Lo JC, Groeger JA, Dijk DJ. Sex differences in the circadian regulation of sleep and waking cognition in humans. Proc Natl Acad Sci USA. 2016;113:E2730–9.
26. Wichmann MW, Zellweger R, DeMaso CM, Ayala A, Chaudry IH. Increased melatonin levels after hemorrhagic shock in male and female C3H/HeN mice. Experientia. 1996;52:587–90.
27. Sato S, Yin C, Teramoto A, Sakuma Y, Kato M. Sexually dimorphic modulation of GABA(A) receptor currents by melatonin in rat gonadotropin-releasing hormone neurons. J Physiol Sci. 2008;58:317–22.
28. Liu Y, Zhou JY, Zhou YH, Wu D, He JL, Han LM, et al. Unique expression of angiotensin type-2 receptor in sex-specific distribution of myelinated Ah-type baroreceptor neuron contributing to sex-dimorphic neurocontrol of circulation. Hypertension. 2016;67:783–91.
29. Qiao GF, Li BY, Lu YJ, Fu YL, Schild JH. 17Beta-estradiol restores excitability of a sexually dimorphic subset of myelinated vagal afferents in ovariectomized rats. Am J Physiol Cell Physiol. 2009;297:C654–64.
30. Qiao GF, Qian Z, Sun HL, Xu WX, Yan ZY, Liu Y, et al. Remodeling of hyperpolarization-activated current, Ih, in Ah-type visceral ganglion neurons following ovariectomy in adult rats. PLoS One. 2013;8:e71184.
31. Wang LQ, Liu SZ, Wen X, Wu D, Yin L, Fan Y, et al. Ketamine-mediated afferent-specific presynaptic transmission blocks in low-threshold and sex-specific subpopulation of myelinated Ah-type baroreceptor neurons of rats. Oncotarget. 2015;6:44108–22.
32. Xu WX, Yu JL, Feng Y, Yan QX, Li XY, Li Y, et al. Spontaneous activities in baroreflex afferent pathway contribute dominant role in parasympathetic neurocontrol of blood pressure regulation. CNS Neurosci Ther. 2018;24:1219–30.
33. Ji Y, Murphy AZ, Traub RJ. Estrogen modulates the visceromotor reflex and responses of spinal dorsal horn neurons to colorectal stimulation in the rat. J Neurosci. 2003;23:3908–15.
34. Liu Y, Zhao SY, Feng Y, Sun J, Lu XL, Yan QX, et al. Contribution of baroreflex afferent pathway to NPY-mediated regulation of blood pressure in rats. Neurosci Bull. 2020;36:396–406.
35. Liu Y, Wu D, Qu MY, He JL, Yuan M, Zhao M, et al. Neuropeptide Y-mediated sex- and afferent-specific neurotransmissions contribute to sexual dimorphism of baroreflex afferent function. Oncotarget. 2016;7:66135–48.
36. Sun J, He C, Yan QX, Wang HD, Li KX, Sun X, et al. Parkinson-like early autonomic dysfunction induced by vagal application of DOPAL in rats. CNS Neurosci Ther. 2021;27:540–51.
37. Liu Y, Wen X, Liu SZ, Song DX, Wu D, Guan J, et al. KCa1.1-mediated frequency-dependent central and peripheral neuromodulation via Ah-type baroreceptor neurons located within nodose ganglia and nucleus of solitary tract of female rats. Int J Cardiol. 2015;185:84–7.
38. Jin YH, Bailey TW, Li BY, Schild JH, Andresen MC. Purinergic and vanilloid receptor activation releases glutamate from separate cranial afferent terminals in nucleus tractus solitarius. J Neurosci. 2004;24:4709–17.
39. Li B, Schild JH. Persistent tetrodotoxin-resistant Na^+ currents are activated by prostaglandin E2 via cyclic AMP-dependent pathway in C-type nodose neurons of adult rats. Biochem Biophys Res Commun. 2007;355:1064–8.
40. Bai Q, Shao J, Cao J, Ren X, Cai W, Su S, et al. Protein kinase C-alpha upregulates sodium channel Nav1.9 in nociceptive dorsal root ganglion neurons in an inflammatory arthritis pain model of rat. J Cell Biochem. 2020;121:768–78.
41. Xu F, Zhong JY, Lin X, Shan SK, Guo B, Zheng MH, et al. Melatonin alleviates vascular calcification and ageing through exosomal miR-204/miR-211 cluster in a paracrine manner. J Pineal Res. 2020;68:e12631.
42. Regrigny O, Delagrange P, Scalbert E, Lartaud-Idjouadiene I, Atkinson J, Chillon JM. Effects of melatonin on rat pial arteriolar diameter in vivo. Br J Pharmaol. 1999;127:1666–70.
43. Zhang Y, Li H, Pu Y, Gong S, Liu C, Jiang X, et al. Melatonin-mediated inhibition of Purkinje neuron P-type Ca^{2+} channels in vitro induces neuronal hyperexcitability through the phosphatidylinositol 3-kinase-dependent protein kinase C delta pathway. J Pineal Res. 2015;58:321–34.
44. Kawashima K, Nagakura A, Wurzburger RJ, Spector S. Melatonin in serum and the pineal of spontaneously hypertensive rats. Clin Exp Hypertens A. 1984;6:1517–28.
45. Cagnacci A, Cannoletta M, Renzi A, Baldassari F, Arangino S, Volpe A. Prolonged melatonin administration decreases nocturnal blood pressure in women. Am J Hypertens. 2005;18:1614–8.
46. Simko F, Paulis L. Melatonin as a potential antihypertensive treatment. J Pineal Res. 2007;42:319–22.
47. Browning C, Beresford I, Fraser N, Giles H. Pharmacological characterization of human recombinant melatonin mt(1) and MT(2) receptors. Br J Pharmacol. 2000;129:877–86.
48. Nishi EE, Almeida VR, Amaral FG, Simon KA, Futuro-Neto HA, Pontes RB, et al. Melatonin attenuates renal sympathetic overactivity and reactive oxygen species in the brain in neurogenic hypertension. Hypertens Res. 2019;42:1683–91.
49. Li JN, Li XL, He J, Wang JX, Zhao M, Liang XB, et al. Sex- and afferent-specific differences in histamine receptor expression in vagal afferents of rats: a potential mechanism for sexual dimorphism in prevalence and severity of asthma. Neuroscience. 2015;303:166–77.
50. Wang LQ, Qian Z, Ma HL, Zhou M, Li HD, Cui CP, et al. Estrogen-dependent KCa1.1 modulation is essential for retaining neuroexcitation of female-specific subpopulation of myelinated Ah-type baroreceptor neurons in rats. Acta Pharmacol Sin. 2021;42:2173–80.
51. Li BY, Feng B, Tsu HY, Schild JH. Unmyelinated visceral afferents exhibit frequency dependent action potential broadening while myelinated visceral afferents do not. Neurosci Lett. 2007;421:62–6.
52. Li BY, Glazebrook P, Kunze DL, Schild JH. KCa1.1 channel contributes to cell excitability in unmyelinated but not myelinated rat vagal afferents [Research Support, N.I.H., Extramural]. Am J Physiol Cell Physiol. 2011;300:C1393–403.
53. Xu Z, Wu Y, Zhang Y, Zhang H, Shi L. Melatonin activates BKCa channels in cerebral artery myocytes via both direct and MT receptor/PKC-mediated pathway. Eur J Pharmacol. 2018;842:177–88.